The rate of ecological acclimation is the dominant uncertainty in long-term projections of a key ecosystem service

Andrew J. Felton[1*], Robert K. Shriver[1,2*], Michael Stemkovski[3], John B. Bradford[4], Katharine N. Suding[5], and Peter B. Adler[1*§]

[1] Department of Wildland Resources and the Ecology Center, Utah State University, Logan, UT 84333, USA
[2] Department of Natural Resources and Environmental Science, University of Nevada, Reno, NV, 89557, USA
[3] USU Biology
[4] US Geological Survey, Southwest Biological Science Center, Flagstaff, AZ, 86001, USA
[5] Department of Ecology and Evolutionary Biology, and Institute of Alpine and Arctic Research, University of Colorado, Boulder, CO 80309, USA
*These authors contributed equally.
[§]Corresponding author

Summary

The potential for ecosystems to continue providing society with essential services may depend on their ability to acclimate to climate change through multiple processes operating from cells to landscapes[1]. While models to predict climate change impacts on ecosystem services often consider uncertainty among greenhouse gas emission scenarios or global circulation models (GCMs)[2,3], they rarely consider the rate of ecological acclimation, which depends on decadal-scale processes such as species turnover[4,5]. Here we show that uncertainty due to the unknown rate of ecological acclimation is larger than other sources of uncertainty in late-century projections of forage production in US rangelands. Combining statistical models fit to historical climate data and remotely-sensed estimates of herbaceous productivity with an ensemble of GCMs, we projected changes in forage production using two approaches. The time-series approach, which assumes minimal acclimation, projects widespread decreases in forage production. The spatial gradient approach, which assumes ecological acclimation keeps pace with climate, predicts widespread increases in forage production. This first attempt to quantify the magnitude of a critical uncertainty emphasizes that better understanding of ecological acclimation is essential to improve long-term forecasts of ecosystem services, and shows that management to facilitate ecological acclimation[6] may be necessary to maintain ecosystem services at historical baselines.

Rapid anthropogenic climate change is disrupting the predictable relationships between climate and ecosystem structure and function that have developed over millenia[7,8]. Ecosystems are responding to this disruption through mechanisms spanning a wide range of time scales. Individual physiological rates can change on scales of minutes to hours, while population sizes and community composition typically change over years to decades, and species colonization and extinction events, as well as evolutionary change, alteration of disturbance regimes, and the

adjustment of biogeochemical cycles may play out over decades, centuries, or longer[9]. We use the term "ecological acclimation" to describe the combined effect of all these responses pushing ecosystem structure and function towards a stochastic equilibrium with climate.

While the fast components of ecological acclimation, such as physiological adjustment, can be studied using experimental and observational approaches, we know much less about the rate of slow components. Experiments typically lack the spatial or temporal extent to observe species turnover or evolutionary adaptation, and may only capture transient behavior[10–12]. Paleoecological observations provide much of what we know about long-term ecological responses to environmental change[13], but the data have critical gaps[15–17], and current rates and magnitudes of warming exceed those observed in the past[18,19]. As a result, the slow processes driving ecological acclimation are a major source of uncertainty in projecting long-term impacts of climate change on ecosystem services[4,5,10]. For example, projections of forest carbon storage derived from ecosystem models differ dramatically because of different assumptions about how the magnitude of the CO_2 fertilization effect may change over the next century[14]. Without relevant empirical data, most ecological models assume either no ecological acclimation or rates of acclimation that perfectly track climate change (e.g., species distribution models). Either way, these models rarely test the sensitivity of their results to these assumptions. Although uncertainty about the rate of ecological acclimation has been recognized[20–23], to our knowledge its magnitude, and its consequences for ecosystem services, remains unknown.

Here, we quantify how varying assumptions about the rates of the slow components of ecological acclimation translates into uncertainty in long-term projections of a key ecosystem service. We compare this uncertainty to uncertainties from more commonly studied sources, such as variation in greenhouse gas emission scenarios (referred to as relative concentration pathways or RCPs) and global circulation models (GCMs), spatial variation, and model parameter error. Our approach exploits differences in how an ecosystem service, rangeland forage production, responds to spatial and temporal variation in climate[24,25]. Studies of regional, spatial relationships between forage production and climate across many sites capture an advanced stage of ecological acclimation: species composition, disturbance regimes, and resource pools have had centuries to equilibrate to a relatively stationary climate[26]. When we project future production based on these spatial gradients, we effectively assume no lags in temporal responses, meaning that even the slow components of ecological acclimation instantaneously track the rate of climate change. A projection based on this assumption represents an empirical upper-bound on the rate of ecological acclimation. In contrast, when we study the relationship between historical interannual variation in weather and interannual variation in production at one location, species composition and resource supply rates are held relatively constant and the slow processes of ecological acclimation are excluded[27]. Projections of future forage production based on this time-series approach represent a scenario of minimal ecological acclimation driven only by mechanisms operating on fine time scales. Together, the spatial gradient, "rapid acclimation" scenario and the time-series, "minimal acclimation" scenario provide objective bounds on the range of uncertainty in future forage production resulting from different assumptions about the rate of ecological acclimation.

We implemented this approach by fitting statistical models to 30 years of remotely-sensed estimates of annual forage production[28] for six extensive rangeland ecoregions in the western U.S. (Extended Data Fig. 1). These data allowed us to simultaneously describe how productivity responds to spatial gradients in climate and temporal variation in weather by decomposing precipitation and temperature observations into spatial and temporal components. The spatial component is represented by variation in mean precipitation and temperature across sites (pixels), while the temporal component is represented by annual anomalies from the mean precipitation and temperature at each site. Because our statistical model contains both spatial and temporal relationships between climate and productivity, we can use either the time-series or spatial gradient approach to project effects of climate change on forage production, depending on the reference period we use to calculate climate means and annual anomalies (Extended Data Fig. 2).

The time-series approach, which holds constant the slow components of ecological acclimation such as species turnover and changes in soil processes, and the spatial gradient approach, which assumes very rapid acclimation, projected dramatically different patterns of forage production changes by late century (2061-2100) (Fig. 1). The time-series approach projected widespread declines in forage production across western US rangelands, with the exception of modest increases for California Annual Grasslands and small portions of the Cold Deserts and Northern Mixed Prairies bordering the Northern Rockies. The projected declines were greatest in the shortgrass steppe and the hot desert ecoregions (in some locations production was projected to decline more than 100% due to extrapolation of linear relationships). In contrast, the spatial gradient approach projected widespread increases in forage production or, at worst, modest

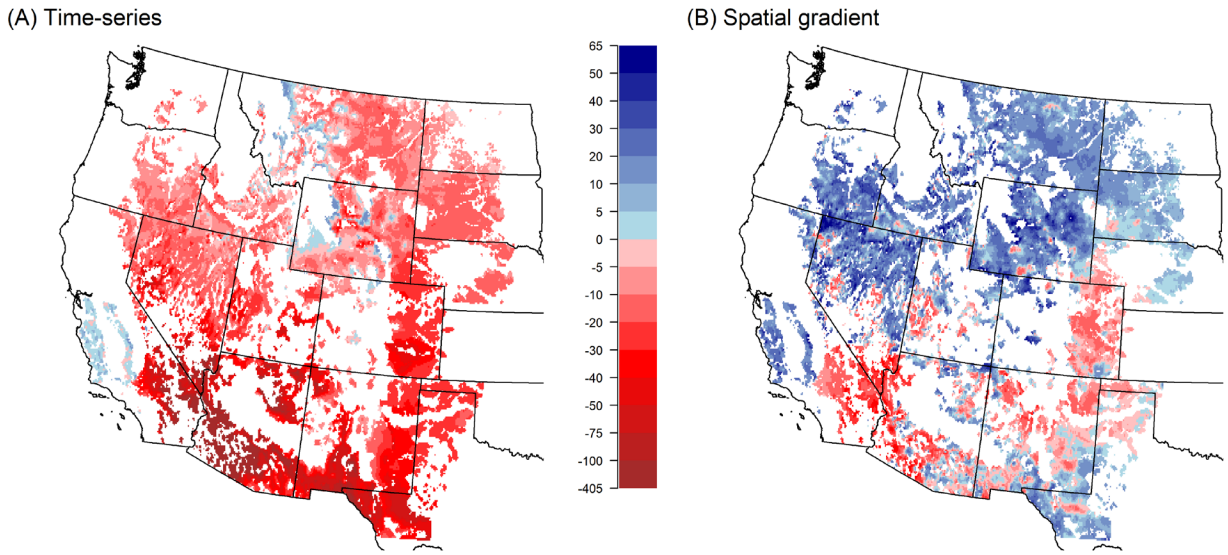

Fig. 1. Projected changes in forage production during the late-century period for the (A) time-series and (B) spatial gradient approaches. Change is expressed as percentage of the historical baseline at each location. Values shown here are means of projections based on 11 GCM

ensemble members for the RCP 8.5 emissions pathway. Areas that are not natural rangeland vegetation were excluded from the analysis, and are shown in white.

decreases. Across 84% of the Cold Deserts and 89% of the Northern Mixed Prairies, projected changes switched from negative under the time-series approach to positive under the spatial gradient approach. For the other ecoregions, the two approaches mostly projected a consistent direction, if not magnitude, of change in forage production, with increases in California and decreases in the Hot Deserts and Shortgrass Steppe.

A sensitivity analysis clarified why differences emerged between the time-series and spatial gradient approaches: positive annual temperature anomalies generally decreased forage production, but spatial variation in mean annual temperature had weak effects (Fig. 2). Essentially, production decreases during hot years but not necessarily in hot locations in all regions except California, which has a cool, winter-spring growing season. Because the time-series approach represents future temperature increases (Extended Data Fig. 3) as temporal anomalies, it leads to strong negative effects of increasing temperatures, while the spatial gradient approach represents future temperature increase as shifts in mean temperature, which have little impact on production. The contrasting effects of temperature means and anomalies, consistent with a recent study of tree growth[29], matches our intuition that at any given location, an unusually hot year can limit production by creating heat stress[30] or exacerbating water stress[31–33]. In contrast, ecosystems have adapted to spatial variation in mean temperatures through a variety of mechanisms, such as genetic adaptation of dominant species, perhaps via shifts in phenology[34], or through filtering of species composition, as seen in the prevalence of C_4 plants in warm growing season ecoregions and C_3 plants in cool growing season ecoregions[35].

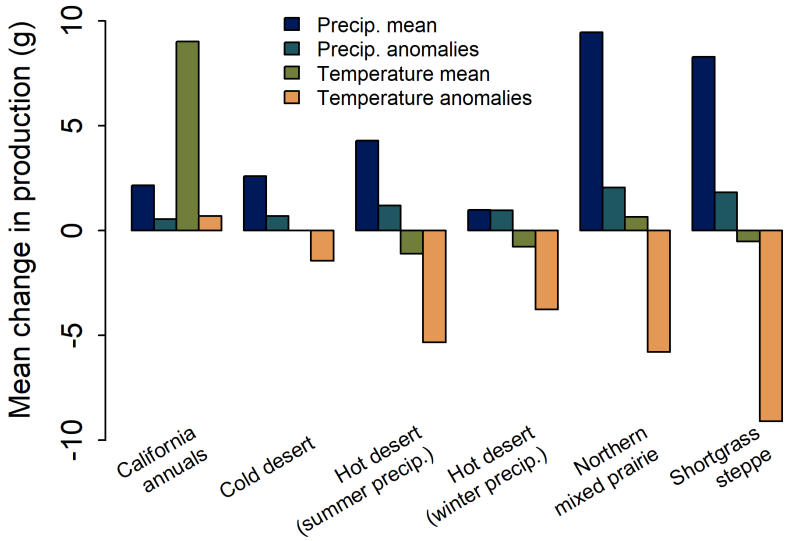

Fig. 2. Sensitivity analysis for the six ecoregion-specific models, indicating key contributions of temperature anomalies over time and precipitation variation across space. Bars show the change in production in late century projections, averaged across each ecoregion, in response to: 1) a 1 cm increase in mean annual precipitation (the influence of spatial variation), 2) a 1 cm

increase in annual precipitation anomalies (the influence of temporal variation), 3) a 1°C increase in mean annual temperature, and 4) a 1°C increase in annual temperature anomalies.

Precipitation sensitivities also contributed to the difference between approaches. Variation in mean annual precipitation had strong positive effects on production in all ecoregions, while precipitation anomalies had much weaker effects (Figure 2), consistent with previous work[36]. In the Cold Deserts and Northern Mixed Prairies, predicted increases in precipitation (Extended Data Fig. 3) had strong positive effects in the spatial gradient approach, offsetting any negative effects of temperature increases, whereas in the time-series approach increasingly positive precipitation anomalies had little effect on production, and the negative effect of temperature anomalies dominated.

The rate of ecological acclimation was the dominant source of uncertainty in projections for five of the six ecoregions (Fig. 3), contributing more than any other single source of uncertainty we considered, which included spatial variation among sites within ecoregions, global circulation models (GCMs), greenhouse gas emission scenarios (RCPs), and model parameter error. The exception was the Hot Desert summer precipitation ecoregion, where spatial variation contributed most to uncertainty. The main effect of acclimation rate plus its two-way interactions with the other sources of uncertainty contributed from 44% (Northern Mixed Prairies) to 54% of the total variation (Hot Deserts with summer precipitation) (Extended Data Table 1). Extended

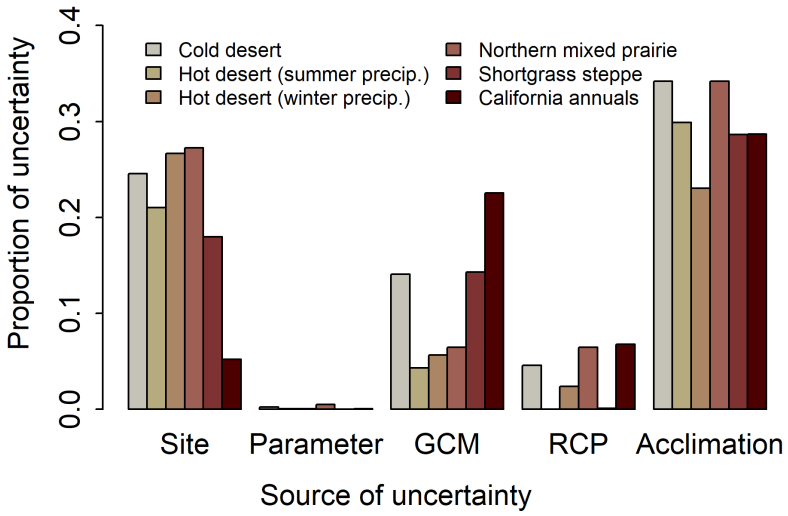

Fig. 3. The rate of ecological acclimation is a large source of uncertainty in projections of future changes in forage production. Uncertainty was partitioned as the proportion of the total sum-of-squares of projected changes in production by late-century. Colors indicate the six ecoregions. Site: spatial variation among remotely sensed pixels with each ecoregion. Parameter: variation among model parameters estimates in the posterior distribution. GCM: variation among global circulation models. RCP: variation among greenhouse gas emission scenarios. Acclimation: variation between the time-series, minimal ecological acclimation, approach and the spatial gradient, rapid acclimation approach.

Data Fig. 4 further emphasizes that variation in projected change among GCMs and RCPs is small relative to the difference between the time-series (minimal acclimation) and the spatial gradient (rapid acclimation) approaches. When we analyzed variation in absolute forage production in the future (Extended Data Fig. 5), rather than relative change, the rate of acclimation still contributed far more to uncertainty than GCMs, RCPs and parameter error, but variation among sites increased (some locations are more productive than others), and process error, which cancels out in the analysis of relative changes, appeared as a major source of uncertainty. What is the rate of ecological acclimation necessary to maintain historical levels of forage production? For some regions, the answer is consistent across the two extreme acclimation scenarios we considered. In the Hot Deserts and Shortgrass Steppe, where GCMs predict decreasing precipitation, our models project production declines even under rapid acclimation. In California, they predict production increases even under minimal ecological acclimation. For many locations in the Cold Deserts and Northern Mixed Prairies, however, the models predict a switch from decreased production under minimal acclimation to increased production under rapid acclimation. To further explore the influence of acclimation on forage production, we considered an intermediate rate of acclimation by using mid-century GCM projections (2021-2060) as the reference for calculating late-century annual anomalies, rather than using historical or late-century reference periods. Median changes in production under this intermediate acclimation scenario were close to zero in the Cold Deserts but were still negative in the Northern Mixed Prairie (Extended Data Fig. 6).

These results suggest that in most locations rapid ecological acclimation may be required to maintain ecosystem services at historical levels. However, research on the slow components of acclimation such as compositional turnover indicates that rapid change is unlikely in rangeland ecosystems. Prolonged drought took eight years to significantly reduce the abundance of the dominant grass in the shortgrass steppe[37]. In the more mesic tallgrass prairie, chronic increases in growing season precipitation took 18 years to change the identity of the dominant to a more productive species[10]. A synthesis of multi-year drought experiments found little evidence of statistical movement away from the time-series model to the spatial gradient model within a decade[38]. On the other hand, extreme events could accelerate this process if they strongly select against species poorly adapted to future conditions[39], though many semiarid systems appear resilient to extreme events such as drought[31]. Paleoecological studies document dramatic compositional changes in the recent past, but cannot provide sub-century resolution[40,41]. However, composition is just one dimension of ecological acclimation. Changes in soil structure and soil resources will also be important, and likely slower to change. For example, recovery of soil organic matter following cultivation can take decades to centuries[42].

Another reason for concern is that our rapid acclimation projections, based on a spatial gradient approach, may be unrealistically optimistic. Transient dynamics could hinder or entirely prevent ecosystem functioning from perfectly track a rapidly changing climate. For example, dispersal limitation could prevent important species from immigrating to a site[43], or a system could be trapped in an unproductive alternative stable state[5], perhaps triggered by biological invasions and altered disturbance regimes[44,45].

Our analysis identifies two important research needs to help society anticipate and mitigate climate-driven changes in ecosystem services. First, we need better information about the rate of ecological acclimation. Other recent studies have also emphasized the need for a better understanding of rates of ecological change[23,46]. We do not need precision; even estimates of such rates to the nearest order of magnitude could greatly reduce the uncertainty of long-term projections such as ours by identifying the appropriate climate reference period, or by informing a model weighting approach[22]. Second, conservation efforts aimed at maintaining ecosystems in their historical states could negatively impact ecosystem services by constraining ecological acclimation[47]. When sustaining ecosystem services is the primary goal, scientists and managers should consider accelerating efforts to facilitate ecological acclimation[6,48], perhaps scaling ideas about assisted migration[49] or applied evolutionary biology[50] to the ecosystem level.

Acknowledgements
This research was supported by the USDA National Institute of Food and Agriculture, Agricultural and Food Research Initiative Competitive Program, Climate and Land Use (grant no. 2018-68002-27923), and by the Utah Agriculture Experiment Station (journal paper #9505). RKS was supported by a Postdoctoral Fellowship (grant no. 2019-67012-29726/project accession no. 1019364) from the USDA National Institute of Food and Agriculture. Any use of trade, firm, or product name is for descriptive purposes only and does not imply endorsement by the U.S. Government. We thank Brady Allred for helping us access the productivity data, and Jonathan Levine, Janneke HilleRisLambers, and Alan Knapp for comments that improved an earlier version of the manuscript.

Author contributions statement
AF, RKS, and PBA designed the study, analyzed data, and drafted portions of the manuscript. JBB and MS contributed to data analysis and writing. KS helped design the study and revise the manuscript.

Data and Code Availability
All data and code needed to reproduce our analysis is available for reviewers at: https://drive.google.com/drive/folders/1Hfu4j7essD728dnkZcjRRUFV-9WrLP6y?usp=sharing
Upon acceptance, these files will be transferred to a permanent digital archive.

References

1. Staudinger, M. D. et al. Impacts of climate change on biodiversity, ecosystems, and ecosystem services: technical input to the 2013 National Climate Assessment. Impacts of climate change on biodiversity, ecosystems, and ecosystem services: technical input to the 2013 National Climate Assessment 296 http://pubs.er.usgs.gov/publication/70039460 (2012).
2. Jiang, J. et al. Forecasting Responses of a Northern Peatland Carbon Cycle to Elevated CO2 and a Gradient of Experimental Warming. Journal of Geophysical Research: Biogeosciences **123**, 1057–1071 (2018).

3. Thomas, R. Q., Jersild, A. L., Brooks, E. B., Thomas, V. A. & Wynne, R. H. A mid-century ecological forecast with partitioned uncertainty predicts increases in loblolly pine forest productivity. Ecological Applications **28**, 1503–1519 (2018).
4. Luo, Y. et al. Coordinated approaches to quantify long-term ecosystem dynamics in response to global change. Global Change Biology **17**, 843–854 (2011).
5. Carpenter, S. Ecological futures: Building an ecology of the long now. Ecology **83**, 2069–2083 (2002).
6. Nelson, E. J. et al. Climate change's impact on key ecosystem services and the human well-being they support in the US. Frontiers in Ecology and the Environment **11**, 483–893 (2013).
7. Blonder, B. et al. Linking environmental filtering and disequilibrium to biogeography with a community climate framework. Ecology **96**, 972–985 (2015).
8. Whittaker, R. H. Communities and ecosystems. (Macmillan, 1975).
9. Smith, M. D., Knapp, A. K. & Collins, S. L. A framework for assessing ecosystem dynamics in response to chronic resource alterations induced by global change. Ecology **90**, 3279–3289 (2009).
10. Collins, S. L. et al. Stability of tallgrass prairie during a 19-year increase in growing season precipitation: Long-term irrigation in native tallgrass prairie. Functional Ecology **26**, 1450–1459 (2012).
11. Reich, P. B., Hobbie, S. E., Lee, T. D. & Pastore, M. A. Unexpected reversal of C_3 versus C_4 grass response to elevated CO_2 during a 20-year field experiment. Science **360**, 317–320 (2018).
12. Seabloom, E. W. et al. Increasing effects of chronic nutrient enrichment on plant diversity loss and ecosystem productivity over time. Ecology **102**, e03218 (2021).
13. Nolan, C. et al. Past and future global transformation of terrestrial ecosystems under climate change. Science **361**, 920–923 (2018).
14. Rollinson, C. R. et al. Emergent climate and CO2 sensitivities of net primary productivity in ecosystem models do not agree with empirical data in temperate forests of eastern North America. Glob Change Biol **23**, 2755–2767 (2017).
15. Williams, J. W., Shuman, B. N., Webb, T., Bartlein, P. J. & Leduc, P. L. Late-quaternary vegetation dynamics in North America: scaling from taxa to biomes. Ecological Monographs **74**, 309–334 (2004).
16. McLachlan, J. S. & Clark, J. S. Reconstructing historical ranges with fossil data at continental scales. Forest Ecology and Management **197**, 139–147 (2004).
17. Jackson, S. T. & Overpeck, J. T. Responses of plant populations and communities to environmental changes of the late Quaternary. pbio **26**, 194–220 (2000).
18. Williams, J. W. & Jackson, S. T. Novel climates, no-analog communities, and ecological surprises. Frontiers in Ecology and the Environment **5**, 475–482 (2007).
19. Steffen, W. et al. Trajectories of the earth system in the Anthropocene. PNAS **115**, 8252–8259 (2018).
20. Keenan, T. F., Davidson, E., Moffat, A. M., Munger, W. & Richardson, A. D. Using model-data fusion to interpret past trends, and quantify uncertainties in future projections, of terrestrial ecosystem carbon cycling. Global Change Biology **18**, 2555–2569 (2012).
21. Luo, Y. & Schuur, E. A. G. Model parameterization to represent processes at unresolved scales and changing properties of evolving systems. Global Change Biology **26**, 1109–1117 (2020).

22. Adler, P. B., White, E. P. & Cortez, M. H. Matching the forecast horizon with the relevant spatial and temporal processes and data sources. Ecography **43**, 1729–1739 (2020).
23. Rollinson, C. R. et al. Working across space and time: nonstationarity in ecological research and application. Frontiers in Ecology and the Environment **19**, 66–72 (2021).
24. Lauenroth, W. K. & Sala, O. E. Long-Term Forage Production of North American Shortgrass Steppe. Ecological Applications **2**, 397–403 (1992).
25. Sala, O. E., Gherardi, L. A., Reichmann, L., Jobbágy, E. & Peters, D. Legacies of precipitation fluctuations on primary production: theory and data synthesis. Phil. Trans. R. Soc. B **367**, 3135–3144 (2012).
26. Sala, O. E., Parton, W. J., Joyce, L. A. & Lauenroth, W. K. Primary Production of the Central Grassland Region of the United States. Ecology **69**, 40–45 (1988).
27. Briggs, J. M. & Knapp, A. K. Interannual variability in primary production in tallgrass prairie: climate, soil moisture, topographic position, and fire as determinants of aboveground biomass. American Journal of Botany **82**, 1024–1030 (1995).
28. Robinson, N. P. et al. Rangeland Productivity Partitioned to Sub-Pixel Plant Functional Types. Remote Sensing **11**, 1427 (2019).
29. Klesse, S. et al. Continental-scale tree-ring-based projection of Douglas-fir growth: Testing the limits of space-for-time substitution. Glob Change Biol **26**, 5146–5163 (2020).
30. Breshears, D. D. et al. Underappreciated plant vulnerabilities to heat waves. New Phytol **231**, 32–39 (2021).
31. Hoover, D. L., Knapp, A. K. & Smith, M. D. Resistance and resilience of a grassland ecosystem to climate extremes. Ecology **95**, 2646–2656 (2014).
32. Diffenbaugh, N. S., Swain, D. L. & Touma, D. Anthropogenic warming has increased drought risk in California. Proc Natl Acad Sci USA **112**, 3931–3936 (2015).
33. Williams, A. P. et al. Large contribution from anthropogenic warming to an emerging North American megadrought. Science **368**, 314–318 (2020).
34. Rice, K. J., Black, R. A., Radamaker, G. & Evans, R. D. Photosynthesis, Growth, and Biomass Allocation in Habitat Ecotypes of Cheatgrass (Bromus tectorum). Functional Ecology **6**, 32–40 (1992).
35. Edwards, E. J. & Still, C. J. Climate, phylogeny and the ecological distribution of C4 grasses. Ecol Letters **11**, 266–276 (2008).
36. Huxman, T. E. et al. Convergence across biomes to a common rain-use efficiency. Nature **429**, 651–654 (2004).
37. Evans, S. E., Byrne, K. M., Lauenroth, W. K. & Burke, I. C. Defining the limit to resistance in a drought-tolerant grassland: long-term severe drought significantly reduces the dominant species and increases ruderals: Grassland response to long-term drought. Journal of Ecology **99**, 1500–1507 (2011).
38. Estiarte, M. et al. Few multiyear precipitation-reduction experiments find a shift in the productivity-precipitation relationship. Glob Change Biol **22**, 2570–2581 (2016).
39. Pérez-Navarro, M. Á. et al. Extreme drought reduces climatic disequilibrium in dryland plant communities. Oikos **130**, 680–690 (2021).
40. Seddon, A. W., Macias-Fauria, M. & Willis, K. J. Climate and abrupt vegetation change in Northern Europe since the last deglaciation. The Holocene **25**, 25–36 (2015).
41. Mottl, O. et al. Global acceleration in rates of vegetation change over the past 18,000 years. Science **372**, 860–864 (2021).

42. Burke, I. C., Lauenroth, W. K. & Coffin, D. P. Soil Organic Matter Recovery in Semiarid Grasslands: Implications for the Conservation Reserve Program. Ecological Applications **5**, 793–801 (1995).
43. Urban, M. C., Tewksbury, J. J. & Sheldon, K. S. On a collision course: competition and dispersal differences create no-analogue communities and cause extinctions during climate change. Proceedings of the Royal Society of London B: Biological Sciences **279**, 2072–2080 (2012).
44. Nagy, R. C. et al. A synthesis of the effects of cheatgrass invasion on US Great Basin carbon storage. Journal of Applied Ecology **58**, 327–337 (2021).
45. Higuera, P. E. & Abatzoglou, J. T. Record-setting climate enabled the extraordinary 2020 fire season in the western United States. Glob. Change Biol. **27**, 1–2 (2021).
46. Williams, J. W., Ordonez, A. & Svenning, J.-C. A unifying framework for studying and managing climate-driven rates of ecological change. Nat Ecol Evol **5**, 17–26 (2021).
47. Fisichelli, N. A., Schuurman, G. W. & Hoffman, C. H. Is 'Resilience' Maladaptive? Towards an Accurate Lexicon for Climate Change Adaptation. Environmental Management **57**, 753–758 (2016).
48. Schuurman, G. W. et al. Resist-accept-direct (RAD)-A framework for the 21st-century natural resource manager. Resist-accept-direct (RAD)-A framework for the 21st-century natural resource manager vol. 2020/2213 http://pubs.er.usgs.gov/publication/70217053 (2020).
49. McLachlan, J., Hellmann, J. J. & Schwartz, M. W. A Framework for Debate of Assisted Migration in an Era of Climate Change. Conservation Biology **21**, 297–302 (2007).
50. Carroll, C., Lawler, J. J., Roberts, D. R. & Hamann, A. Biotic and Climatic Velocity Identify Contrasting Areas of Vulnerability to Climate Change. PLOS ONE **10**, e0140486 (2015).
51. Kuchler, A. W. Potential Natural Vegetation of the Conterminous United States. American Geographical Society **Special Publication No. 36**, (1964).
52. Felton, A. J. et al. Biotic versus abiotic controls on temporal sensitivity of primary production to precipitation across North American drylands. New Phytologist **n/a**, (2021).
53. Livneh, B. et al. A spatially comprehensive, hydrometeorological data set for Mexico, the U.S., and Southern Canada 1950–2013. Sci Data **2**, 150042 (2015).
54. Livneh, B. et al. A Long-Term Hydrologically Based Dataset of Land Surface Fluxes and States for the Conterminous United States: Update and Extensions. J. Climate **26**, 9384–9392 (2013).
55. Tredennick, A. T., Hooker, G., Ellner, S. P. & Adler, P. B. A practical guide to selecting models for exploration, inference, and prediction in ecology. Ecology (2021) doi:10.1002/ecy.3336.
56. Bradford, J. B., Schlaepfer, D. R. & Lauenroth, W. K. Ecohydrology of Adjacent Sagebrush and Lodgepole Pine Ecosystems: The Consequences of Climate Change and Disturbance. Ecosystems **17**, 590–605 (2014).
57. Schlaepfer, D. R. & Andrews, C. A. rSFSW2: Simulation Framework for SOILWAT2. (2018).
58. Kleinhesselink, A. R. & Adler, P. B. The response of big sagebrush (Artemisia tridentata) to interannual climate variation changes across its range. Ecology **99**, 1139–1149 (2018).
59. Tredennick, A. T. et al. Forecasting climate change impacts on plant populations over large spatial extents. Ecosphere **7**, (2016).
60. Hooten, M. B. & Hefley, T. J. Bringing Bayesian Models to Life. (CRC Press, 2019).

61. Moss, R. H. et al. The next generation of scenarios for climate change research and assessment. Nature **463**, 747–756 (2010).
62. Taylor, K. E., Stouffer, R. J. & Meehl, G. A. An Overview of CMIP5 and the Experiment Design. Bulletin of the American Meteorological Society **93**, 485–498 (2012).
63. Knutti, R., Masson, D. & Gettelman, A. Climate model genealogy: Generation CMIP5 and how we got there. Geophysical Research Letters **40**, 1194–1199 (2013).
64. Rupp, D. E., Abatzoglou, J. T., Hegewisch, K. C. & Mote, P. W. Evaluation of CMIP5 20th century climate simulations for the Pacific Northwest USA. Journal of Geophysical Research: Atmospheres **118**, 10,884-10,906 (2013).
65. Maurer, E. P., Brekke, L., Pruitt, T. & Duffy, P. B. Fine-resolution climate projections enhance regional climate change impact studies. Eos Trans. AGU **88**, 504–504 (2007).

Methods

Rangeland ecoregions

We studied five expansive rangeland ecoregions of the western United States: the Northern Mixed Prairies (NM), the Shortgrass Steppe (SGS), the Cold Deserts (CD), the California Annual grasslands (CA), and the Hot Deserts (a combination of the Mojave, Sonoran, and Chihuahuan Deserts). These ecoregions were defined by a map of potential natural vegetation[51]. A previous assessment of remotely-sensed functional type cover in each of these ecoregions was consistent with expectations based on potential natural vegetation[52]. We split the Hot Deserts ecoregion into two to account for differences in precipitation and growing season timing. We assigned sites receiving > 30% of total annual precipitation during the summer months (July-September) to a Hot Desert summer precipitation (HDS) ecoregion, and assigned sites receiving less than 30% of annual precipitation during summer to a Hot Desert winter precipitation ecoregion (HDW) (Extended Data Fig. 1).

Forage production data

We leveraged a spatiotemporal remotely-sensed dataset of annual net primary productivity data developed specifically for rangeland ecosystems of the western US, spanning the years 1986-2015[28]. This data product partitions annual (calendar year) vegetation productivity (defined as net carbon inputs in g/m^2) into functional groups of shrubs, trees, annual forbs/grasses, and perennial forbs grasses. We defined annual forage production, our response variable, as the sum of productivity from the herbaceous functional groups: annual and perennial grasses and forbs. We aggregated these data from their native spatial resolution (30 m) to $1/16^{th}$ degree (approximately 6.9 km) to match the spatial resolution of the historical climate data and cropped the data by the spatial extent of each of the six ecoregions.

After aggregation, we applied a multi-step filtering process to remove non-rangeland pixels, such as irrigated agriculture[52]. We first removed pixels where less than 50% of 30 m pixels were used for aggregation to the 6.9 km resolution. We also removed pixels where the average net primary productivity was below 10 g/m^2. We then sequentially removed outlier pixels for each ecoregion based on distributions of multiple metrics of plant-water relationships across each ecoregion. These metrics, presented in order, included 1) mean precipitation use efficiency (mean net primary productivity/mean annual precipitation), the slope of annual productivity and annual precipitation, and 3) annual precipitation use efficiency. Outliers were defined as beyond three standard deviations from the mean. After filtering, we had 774 pixels in California Annual grasslands, 13,869 in Cold Desert, 6,446 in Hot Deserts (summer precipitation), 1,573 in Hot Deserts (winter precipitation), 13,070 in the Northern Mixed Prairie, and 4,925 in the Shortgrass Steppe.

Historical climate data and model selection

For historical climate data, we used a gridded hydrometeorological data product with daily time steps of temperature and precipitation[53,54]. The native resolution of these data are ~6 km, but

were aggregated to 6.9 km to match the resolution of soil moisture data used in our pre-model fitting. These data encompass years 1915-2015, but here we focus on years 1986-2015 to correspond with the temporal coverage of the forage production data.

Explaining an annual ecological response, like production, using daily weather data poses a difficult model selection problem because of the virtually limitless choices about how to aggregate the weather data[55]. Therefore, we constrained our covariate selection approach in two ways: First, in every model we considered only one variable representing moisture stress and one variable representing heat stress, along with their interactions as explained below. This constraint guarded against collinearity and overfitting. In addition to precipitation (moisture stress) and temperature (heat stress), we considered additional covariates simulated by the SOILWAT ecohydrological model[56,57] , using the daily weather data[54,54] as input for each location (pixel). These included moisture-related variables such as soil water availability, volumetric water content, and transpiration, and variables related to heat stress such as potential evapotranspiration (PET) and the ratio of soil water availability to PET. Preliminary analyses using linear mixed effects models (not shown) indicated that precipitation and temperature explained more variation in observed productivity than pairs of variables derived from SOILWAT. For all subsequent models reported here, the raw covariates were precipitation and temperature.

Second, we constrained variable selection using our *a priori* knowledge of each ecoregion to define the most relevant climate window, rather than exhaustively searching for the optimal temporal window over which to aggregate the moisture stress and heat stress variables. In general, these periods coincide with the growing season. For the California annual grasslands, the cold deserts, and the hot deserts with winter precipitation, we summed precipitation and averaged temperature over fall, winter, and spring (October – June). For the northern mixed prairies, shortgrass steppe, and hot deserts receiving summer precipitation, we aggregated over spring and summer (April – September).

While the raw covariates for each ecoregion were total precipitation and mean temperature aggregated over the relevant seasons, we decomposed each of these raw covariates into spatial means and temporal (annual) anomalies and included interactions among them[52,58]. Specifically, we decomposed $P_{i,t}$, the precipitation received in pixel i and year t, into the mean precipitation in pixel i, $\bar{P}_i$, and the annual precipitation anomaly in pixel i and year t, $\delta P_{i,t}$. The key point is that $\bar{P}$ varies only across space while δP varies only in time. Similarly, we define $\bar{T}_i$ as the mean temperature in pixel i and $\delta T_{i,t}$ as the annual temperature anomaly. We then designed interactions among these derived covariates to allow the effects of annual anomalies to vary in space, as shown in Extended Data Table 2. (Note that in our computer code, we refer to the precipitation and temperature anomalies as deviations.)

Model fitting

We developed spatiotemporal hierarchical models for each ecoregion to infer the response of forage production (herbaceous NPP) to past climate conditions, and then used this model to predict changes in forage in response to future climate change.

Observed forage production, *y,* in each pixel, *i,* and year, *t,* was modeled as normally distributed with mean ($\mu_{i,t}$) and process variance ($\sigma^2_{(p)}$):

$$y_{i,t} \sim N(\mu_{i,t}, \sigma^2_{(p)}). \quad [1]$$

The process model for the mean is a linear model of covariates $\mathbf{X}_{i,t}$ and ecoregion-specific parameters **b**, along with additive, pixel-specific spatial (η_i) and year-specific temporal (τ_t) random effects:

$$\mu_{i,t} = \mathbf{X}_{i,t}\mathrm{b} + \eta_i + \tau_t. \quad [2]$$

Year random effects were fit with a non-centered parameterization (more computationally efficient in Stan) using a standard normal distribution, rescaled with standard deviation $\sigma_{(t)}$:

$$\tau_t = \tau'_t * \sigma_{(t)} \quad [3]$$

$$\tau'_t \sim N(0,1). \quad [4]$$

Spatial random effects were fit using a spatial dimension reduction approach following the general methods of [59]. Dimension reduction approaches help overcome the computational burden of modeling residual autocorrelation structures by reducing the number of pixels to a constituent number of knots that summarize the landscape of spatially autocorrelated processes not accounted for by covariates. Spatial random effects were modeled as

$$\boldsymbol{\eta} = \mathbf{K} * \boldsymbol{\alpha} \quad [5]$$

where $\boldsymbol{\eta}$ is a vector of spatial random effects specific to each pixel, *i* (i = 1...*I*), $\boldsymbol{\alpha}$ is a vector of spatial random effects specific to each knot, *s* (*s* = 1...*S*), and **K** is an *I* by *S* matrix that describes how the knot based random effects are translated into random effects for each pixel.

Each element in **K,** $K_{i,s}$, is a normalized, distance weighted function from each knot to pixel

$$K_{i,s} = w_{i,s} / \sum_{i=1}^{I} w_{i,s} \quad [6]$$

$$w_{i,s} = exp(-d_{i,s}/\phi) \quad [7]$$

where $d_{i,s}$ is the distance from pixel *i* to knot *k,* and ϕ is a distance decay parameter.

Knot-based random effects were fit with a non-centered parameterization using a standard normal distribution, rescaled with standard deviation $\sigma_{(s)}$ as:

$$\alpha_s = \alpha'_s * \sigma_{(s)} \quad [8]$$

$$\alpha'_s \sim N(0,1). \quad [9]$$

Following the approach of [59], ϕ and knot spacing was determined empirically prior to model fitting to improve computation based on the observed scale of spatial auto-correlation. To do this, we fit a version of our model including only fixed effects, using the maximum likelihood

solution for **b**. We then calculated model residuals between our fixed-effects-only model and observed NPP values, and visualized the scale of autocorrelation using empirical semi-variograms (Extended Data Fig. 7). The spacing of knots is determined visually by the approximate sill distance of each ecoregion, and value of ϕ is one-third the sill distance. Knots were placed in a regular grid across each ecoregion with spacing based on sill distance (Extended Data Fig. 8).

To limit covariate overfitting, we regularized covariates with Bayesian ridge regression. This was done by fitting seven different models in each ecoregion to a subset of the data (randomly withholding 5 years, ~17% of the data) with increasingly wider zero centered priors for covariate parameters ($\mathbf{b} \sim N(0, \mathbf{I}\upsilon^2)$), and then testing the predictive ability of each prior specification with the withheld data [60]. The priors for **b** that minimized the average mean squared predictive error (MSPE) in each ecoregion were then used to fit the final model to the full dataset (Extended Data Fig. 9). For each ecoregion, this final model was used to project future forage production. Parameter estimates are shown in Extended Data Table 3, and goodness-of-fit measures are shown in Extended Data Table 4.

Future climate data

We focus our projections on the late-century time period, defined as 2061-2100. Forage projections were run separately for each of the six ecoregions. To represent the range of uncertainty in future climate data, daily climate data from eleven different general circulation models (GCMs) under two different representative concentration pathways (RCPs) families; scenario 4.5, which represents a relatively low emissions scenario, and scenario 8.5, which represents the highest emissions scenarios[61,62], were used to drive the model. The GCMs were selected both to represent the diversity of model projections among GCMs included in CMIP5[63], and to include models that performed well in hindcast comparisons within the western U.S.[64] (Rupp unpublished data). The 11 GCMs we used were: CESM1-CAM5, CSIRO-Mk3-6-0, CNRM-CM5, FGOALS-g2, FGOALS-s2, GISS-E2-R, HadGEM2-ES, inmcm4, IPSL-CM5A-MR, and MIROC-ESM. Future climate data was extracted as monthly time-series from 1/8° downscaled and bias-corrected products of the fifth phase of the Climate Model Intercomparison Project (CMIP5)[65].

Forage projections and uncertainty and sensitivity analyses

We combined the parameters estimates of the statistical model with GCM simulations of late century precipitation and temperature to project future forage production. The first step was decomposing future precipitation and temperature into means and annual anomalies for each location (pixel) (Extended Data Fig. 2). One option is to calculate future annual anomalies in precipitation and temperature based on the *historical* means at each location. This implements a time-series approach: we assume that climate means will not change, but there will be many hotter than normal years in the future, and the effects of these anomalous years are captured by the model's temporal anomaly terms. The second option is to calculate future annual anomalies based on the *future* means at each location. This implements the spatial gradient approach: we assume relatively small changes in the annual anomalies but potentially large changes in mean

precipitation and temperature, and the effects of these shifts in the means are captured in the model's spatial terms. Although most of our analyses focus on the time-series (historical means as the reference) and spatial gradient (future means as the reference) approaches, we also explored a third option in which we calculate annual anomalies based on GCM projections for the mid-century period (2021-2060). This approach represents an intermediate rate of ecological acclimation.

After calculating the climate covariates, we projected future productivity. For each location and each year in the late century period, we predicted productivity for 22 climate scenarios (11 GCMs × 2 RCPs), 500 sets of model parameters drawn from the MCMC chains, and our two methods (time-series and spatial gradient). We then averaged predicted productivity across years within each pixel, preserving variation among all combinations of locations, parameter draws, GCMs, RCPs, and projection method.

The uncertainty analysis featured in the main text methods focuses on the future change in mean forage production relative to the historical period. We calculated change in a given pixel as the difference between the mean annual production in the future period and mean annual production from the historical period, divided by the historical mean. Note that the historical mean is not based on observed data, but rather on predictions from the statistical model, ensuring that biases in the model do not influence the estimated change in productivity. Dividing by the historical mean led to some very large values in pixels where the historical mean was close to zero. Our uncertainty analysis was sensitive to these outliers, so we removed sites with predicted historical mean production less than 10 g m^{-2} (26 out of 13,839 pixels in the Cold Deserts, 18 of 6,446 pixels in the Hot Deserts with summer precipitation, and 14 of 1,573 pixels in the Hot Deserts with winter precipitation). Because our predictions for the two periods assume the same model process error, process error cannot contribute to change in productivity and we can ignore it. Similarly, we can ignore random year effects, which we assumed have the same variance in the future as in the historical period.

To perform the calculations, we loaded all the projected changes in forage production into an array with the following dimensions: 1) sites, 2) parameters draws from the posterior distribution (500), 3) GCMs (11), 4) RCPs (2), 5) rate of acclimation (2). We then analyzed variation in this array using two approaches. First, we took a sums-of-squares approach, quantifying the proportion of the total sum-of-squares contributed by each of the five main effects (the dimensions of the array), as well as the four two-way interactions involving rate of acclimation. Second, we quantified the standard deviation of the marginal means of each main effect. For example, we calculated the mean change in productivity at each site, averaging over parameters, GCMs, RCPs, and rate of acclimation, then computed the standard deviation among site means as a measure of the variation among sites in projected change in forage production.

We repeated this analysis of standard deviation for variation in absolute forage production, rather than variation in the change in forage production. For this case, we also included variation due to process error and random year effects, as estimated by the statistical models.

Note that results of both the sum-of-squares partitioning and the analysis of standard deviation are affected by the number of levels of each main factor (e.g., sites, parameters, GCMs, RCPs, projection methods). Because we consider only the two extremes for the rate of ecological acclimation, our estimate of the relative contribution from this source represents an upper bound. New information on rates of acclimation could reduce this uncertainty either by moderating the extremes, or by working with objective distributions of rates of acclimation (as we currently do with parameter error).

We also conducted a sensitivity analysis to help us understand the projections. For each ecoregion, we used the point estimates of model parameters to quantify the expected change in production at each pixel caused by 1) adding 1 cm to all mean precipitation values, 2) adding 1 cm to all annual precipitation anomalies, 3) adding 1°C to all mean temperature values, and 4) adding 1°C to all temperature anomalies. These perturbations fall well within the range of expected future changes in precipitation and temperature (Extended Data Fig. 3). We recalculated all interaction terms after each perturbation. We report the mean change across locations for each of these four perturbations.

We performed a final set of projections to represent an intermediate rate of ecological acclimation, using GCM output for mid-century as the reference for calculating each pixel's climate means and annual anomalies for the late-century period. We did not repeat the full uncertainty partitioning, but simply compared the averaged projected change in forage production for each pixel to the average change projected by the time-series (historical climate reference period) and spatial gradient (late-century climate reference period) approaches.